

Gap narrowing in charged and doped silicon nanoclusters

Andrey Titov*

CNRS, IM2NP (UMR 6242), F.S.T., Avenue Escadrille Normandie Niemen, F-13397 Marseille Cedex, France;
 Institut Néel, CNRS-UJF, 25 Avenue des Martyrs BP 166, Grenoble Cedex 9 38042, France;
 and A. M. Prokhorov General Physics Institute, Russian Academy of Sciences, 38 Vavilov Street, Moscow 119991, Russia

Fabienne Michelini† and Laurent Raymond

Aix-Marseille Université, IM2NP; and CNRS, IM2NP (UMR 6242), Faculté des Sciences et Techniques, Campus de Saint-Jérôme,
 Avenue Escadrille Normandie Niemen, F-13397 Marseille Cedex, France

Erkin Kulatov

A. M. Prokhorov General Physics Institute, Russian Academy of Sciences, 38 Vavilov Street, Moscow 119991, Russia

Yurii A. Uspenskii‡

P. N. Lebedev Physical Institute, Russian Academy of Sciences, 53 Avenue Leninskii, Moscow 117924, Russia
 (Received 4 June 2010; revised manuscript received 28 October 2010; published 10 December 2010)

The gap narrowing in charged $\text{Si}_{35}\text{H}_{36}$ and n -type doped $\text{Si}_{34}\text{DH}_{36}$ ($D=\text{P, As, Sb, S, Se, and Te}$) clusters is studied within the GW approximation, including energy dependence of the dielectric matrix and local-field effects. It is shown that the density functional theory does not properly describe the gap narrowing in clusters, as it was found earlier in bulk Si. The main mechanisms of this effect in clusters are the same as in bulk Si: (i) the screened exchange interaction between additional electrons and (ii) the extra screening of the Coulomb interaction by additional electrons. At the same time, our calculations show that the carrier-induced gap narrowing has peculiar features in the clusters. A much weaker screening of the electron-electron interaction strongly increases the first and decreases the second mechanism of gap narrowing in Si clusters as compared to bulk Si. We find also that the gap-narrowing effect is more pronounced in doped clusters than in charged ones due to the charge localization near impurity ions. The electronic spectrum of the charged and doped Si clusters with one electron is spin split. The local-density approximation calculation greatly underestimates the value of the spin splitting. A calculation performed with the screened Hartree-Fock method shows that the splitting is large. It considerably narrows the gap and brings important spin effects into cluster properties.

DOI: [10.1103/PhysRevB.82.235419](https://doi.org/10.1103/PhysRevB.82.235419)

PACS number(s): 73.22.-f, 73.21.La, 71.20.Mq

I. INTRODUCTION

Additional electrons introduced into a nanocrystal by impurity doping or injected by an applied voltage may cause important changes in its electronic structure and, in particular, significant gap narrowing. Development of the floating-gate flash-memory elements, where nanocrystals are imbedded into the gate oxide of a metal-oxide-semiconductor field-effect-transistor (MOS FET) to trap electrons,¹ is a reason of practical interest to the effects of high electron concentration on the gap. The effect of gap narrowing has been extensively studied in semiconductors over last decades. In doped bulk silicon the gap renormalization was observed in electrical,² photoluminescence,³ and optical-absorption⁴ experiments. Theoretical investigations within different approximations were also performed^{5–8} and basic mechanisms of the effect in bulk semiconductors were identified. All these investigations conclude that the gap narrowing in semiconductors is essentially a many-body effect and it is caused by a modification of the electron-electron interactions induced by the additional electrons. This effect cannot be properly evaluated from the Kohn-Sham gap narrowing, calculated within the local-density approximation (LDA). The experimentally observed quasiparticle gap, as well as the effect of the gap narrowing, are rather precisely described by the quasiparticle theory within the GW approximation (GWA).

A well-controlled electron charging of a quantum dot can be realized by electron injection from electric contacts⁹ or from a scanning-tunnel-microscope tip.¹⁰ Simultaneous charging and photoluminescence measurements in InAs self-assembled quantum dots were reported in Ref. 11. In such measurements optical transitions between conduction and valence states in charged quantum dots are detected. Effects of the electron charging in quantum dots were also studied by optical-absorption spectroscopy.¹² Theoretically the question of the gap renormalization in charged quantum dots was considered within the Hartree-Fock (HF) approximation.¹³ A redshift of emission lines in CdSe quantum dots was calculated using a screened Hartree-Fock exchange with a static dielectric constant.¹⁴ A study of the gap narrowing in bulk silicon performed with the GWA (Ref. 8) shows that energy dependence of the dielectric function is important for the correct effect description. In this paper we study the gap narrowing in charged and doped silicon nanocrystals within the GWA, computing the full dynamic dielectric matrix. We suppose that the electron wave functions in charged clusters are only slightly modified by the charging, therefore the gap narrowing is treated in the first-order perturbation theory. These results are compared to gap narrowing calculated in clusters doped with single and double donors.

The remainder of the paper is organized as follows. The calculation method of gap narrowing in charged and doped

clusters is described in Sec. II. An *ab initio* calculation of the gap narrowing in bulk silicon is given in Sec. III, where basic mechanisms of the gap narrowing in bulk semiconductors are discussed. Results obtained for charged and doped clusters are presented in Sec. IV and discussed in Sec. V.

II. COMPUTATIONAL METHODS

Electronic states in bulk silicon and silicon clusters were calculated within the Hedin's GW approximation¹⁵ using the ABINIT code.¹⁶ The supercell approach and periodic boundary conditions were applied in the case of silicon clusters. A supercell based on primitive translations of the cubic face-centered lattice with a silicon cluster inside was constructed in order to obtain electronic states of isolated clusters. The lattice parameter of the supercell was chosen sufficiently large to ensure a good vacuum separation between clusters in neighbor supercells. The primitive cell of the diamond crystal structure, containing two atoms, was used to calculate the band structure of bulk silicon.

The first step of our calculation is the solution of the LDA Kohn-Sham equations for the eigenfunctions ϕ_{nk}^{LDA} and eigenvalues E_{nk}^{LDA}

$$\left[-\frac{1}{2}\nabla^2 + V_{\text{ext}}(\mathbf{r}) + V_H(\mathbf{r}) + V_{xc}(\mathbf{r}) \right] \phi_{nk}^{\text{LDA}}(\mathbf{r}) = E_{nk}^{\text{LDA}} \phi_{nk}^{\text{LDA}}(\mathbf{r}), \quad (1)$$

where V_H is the average (Hartree) Coulomb potential of electrons and the external potential V_{ext} is due to ions and may contain a contribution from charges disposed out of the cluster (the Hartree atomic units $\hbar = m_e = e = 1$ are used here and throughout the paper). In our calculation V_{ext} is described by the Troullier-Martin norm-conserving pseudopotentials¹⁷ of atoms generated by Khein and Allan.^{18,19} Exchange and correlation effects within the LDA are included into the equations through the potential V_{xc} . An occupation broadening scheme²⁰ with a small smearing parameter was applied during iterations to self-consistency in Eq. (1) and electron occupation factors f_{nk} for each $n\mathbf{k}$ state were determined. It should be noted that the Kohn-Sham eigenvalues obtained from Eq. (1) have no formal justification as quasiparticle energies. In most metals these eigenvalues are rather close to observed quasiparticle energies while in semiconductors and insulators the Kohn-Sham gap values found from Eq. (1) are typically underestimated, as compared to gap values obtained in experiment. An adequate ground for the description of electronic excitations in solids is given by the concept of quasiparticles, which provides fairly good estimates of experimental gap in semiconductors and insulators.^{21,22} The quasiparticle wave functions ϕ_{nk}^{QP} and energies E_{nk}^{QP} are obtained by solving the equation

$$\left[-\frac{1}{2}\nabla^2 + V_{\text{ext}}(\mathbf{r}) + V_H(\mathbf{r}) \right] \phi_{nk}(\mathbf{r}) + \int \Sigma(\mathbf{r}, \mathbf{r}', E_{nk}) \phi_{nk}(\mathbf{r}') d\mathbf{r}' = E_{nk} \phi_{nk}(\mathbf{r}). \quad (2)$$

The self-energy operator Σ , which is generally nonlocal,

energy-dependent, and non-Hermitian, takes into account the exchange and correlation effects. Following early quasiparticle calculations^{21,22} the operator $\Sigma - V_{xc}$ is treated in Eq. (2) as a perturbation to the Hamiltonian Eq. (1). In the first order of the perturbation theory the quasiparticle eigenvalues are given by

$$E_{nk}^{\text{QP}} = E_{nk}^{\text{LDA}} + \int \phi_{nk}^{\text{LDA}*}(\mathbf{r}_1) Z_{nk} \times [\Sigma(\mathbf{r}_1, \mathbf{r}_2, E_{nk}^{\text{LDA}}) - V_{xc}(\mathbf{r}_1) \delta(\mathbf{r}_1 - \mathbf{r}_2)] \times \phi_{nk}^{\text{LDA}}(\mathbf{r}_2) d\mathbf{r}_1 d\mathbf{r}_2, \quad (3)$$

where Z_{nk} is the quasiparticle renormalization factor²¹⁻²³

$$Z_{nk}^{-1} = 1 - \int \phi_{nk}^{\text{LDA}*}(\mathbf{r}_1) \times \left[\frac{\partial \Sigma(\mathbf{r}_1, \mathbf{r}_2, E)}{\partial E} \Big|_{E_{nk}^{\text{LDA}}} \right] \phi_{nk}^{\text{LDA}}(\mathbf{r}_2) d\mathbf{r}_1 d\mathbf{r}_2. \quad (4)$$

The self-energy operator Σ in Eq. (3) and (4) calculated within the GWA is given by

$$\Sigma(\mathbf{r}_1, \mathbf{r}_2, E) = \frac{i}{2\pi} \int_{-\infty}^{+\infty} W(\mathbf{r}_1, \mathbf{r}_2, E') \times G(\mathbf{r}_1, \mathbf{r}_2, E + E') e^{iE'\eta} dE'. \quad (5)$$

The one-particle Green's function $G(\mathbf{r}_1, \mathbf{r}_2, E)$

$$G(\mathbf{r}_1, \mathbf{r}_2, E) = \sum_{n\mathbf{k}} \left[\frac{\phi_{n\mathbf{k}}^{\text{LDA}}(\mathbf{r}_1) \phi_{n\mathbf{k}}^{\text{LDA}*}(\mathbf{r}_2) f_{n\mathbf{k}}}{E - E_{n\mathbf{k}}^{\text{LDA}} - i\eta} + \frac{\phi_{n\mathbf{k}}^{\text{LDA}}(\mathbf{r}_1) \phi_{n\mathbf{k}}^{\text{LDA}*}(\mathbf{r}_2) (1 - f_{n\mathbf{k}})}{E - E_{n\mathbf{k}}^{\text{LDA}} + i\eta} \right] \quad (6)$$

contains the eigenfunctions ϕ_{nk}^{LDA} , eigenvalues E_{nk}^{LDA} and electron occupation factors f_{nk} obtained in the self-consistent LDA calculation, η is a positive infinitesimal, a value 0.05 eV for η was used in all calculations. The screened Coulomb interaction W in Eq. (5) can be developed in a Fourier series

$$W(\mathbf{r}_1, \mathbf{r}_2, E) = \frac{1}{\Omega} \sum_{\mathbf{q}, \mathbf{G}_1, \mathbf{G}_2} e^{i(\mathbf{q} + \mathbf{G}_1)\mathbf{r}_1} W_{\mathbf{G}_1, \mathbf{G}_2}(\mathbf{q}, E) e^{-i(\mathbf{q} + \mathbf{G}_2)\mathbf{r}_2}, \quad (7)$$

where \mathbf{G}_1 and \mathbf{G}_2 are reciprocal lattice vectors, \mathbf{q} is a wave vector in the first Brillouin zone, Ω is the supercell volume. The Fourier coefficients of the screened Coulomb potential W are given by

$$W_{\mathbf{G}_1, \mathbf{G}_2}(\mathbf{q}, E) = \epsilon_{\mathbf{G}_1, \mathbf{G}_2}^{-1}(\mathbf{q}, E) v(\mathbf{q} + \mathbf{G}_1), \quad (8)$$

where $\epsilon_{\mathbf{G}_1, \mathbf{G}_2}^{-1}(\mathbf{q}, E)$ are Fourier elements of the inverse dielectric function, $v(\mathbf{q}) = 4\pi/|\mathbf{q}|^2$ is Fourier transform of the Coulomb interaction. The energy dependence of the inverse dielectric function was fitted to the plasmon-pole form

$$\epsilon_{\mathbf{G}_1, \mathbf{G}_2}^{-1}(\mathbf{q}, E) = \delta_{\mathbf{G}_1, \mathbf{G}_2} + \frac{\Omega_{\mathbf{G}_1, \mathbf{G}_2}^2}{E^2 - \omega_{\mathbf{G}_1, \mathbf{G}_2}^2}. \quad (9)$$

The matrix elements $\epsilon_{\mathbf{G}_1, \mathbf{G}_2}^{-1}(\mathbf{q}, E)$ of the inverse dielectric matrix were calculated at two energies $E=0$ and $E=16.7i$ eV using the Adler-Wiser formulation.^{24,25} The Eq. (9) was then solved for the plasmon-pole parameters $\Omega_{\mathbf{G}_1, \mathbf{G}_2}$ and $\omega_{\mathbf{G}_1, \mathbf{G}_2}$. The inverse dielectric matrix Eq. (9) is energy dependent and includes local-field effects; it was used in Eq. (8) to construct the screened interaction W .

The quasiparticle eigenvalues $E_{n\mathbf{k}}^{\text{QP}}$ of initial and n -type doped clusters were obtained from Eq. (3). The gap of the initial cluster was determined as the energy difference between the quasiparticle energies of the lowest unoccupied and the highest fully occupied states. The same states were considered in order to determine the gap in doped clusters although the lowest unoccupied state, being empty in the initial cluster, is partially or fully occupied in the doped clusters. In order to operate unified terms for initial, charged and doped clusters, we shall refer the lowest unoccupied and highest occupied states determined in the initial cluster as the lowest conduction (LC) and highest valence (HV) states, respectively. The gap narrowing upon doping is calculated as a the difference between gaps of doped and initial clusters

$$\Delta E_G = E_G^{\text{doped}} - E_G^{\text{initial}}. \quad (10)$$

The gap narrowing in charged clusters was obtained as a difference between shifts of the lowest conduction and highest valence states upon charging

$$\Delta E_G = \Delta E_{\text{LC}} - \Delta E_{\text{HV}}. \quad (11)$$

The shifts ΔE_{LC} and ΔE_{HV} in first order perturbation theory are due to the change in the Hartree V_H , exchange-correlation V_{xc} potentials, renormalization factor $Z_{n\mathbf{k}}$, and self-energy operator Σ upon electron charging

$$\begin{aligned} \Delta E_{n\mathbf{k}}^{\text{QP}} = & \int \phi_{n\mathbf{k}}^{\text{LDA}*}(\mathbf{r}) \Delta V_H(\mathbf{r}) \phi_{n\mathbf{k}}^{\text{LDA}}(\mathbf{r}) d\mathbf{r} + \int \phi_{n\mathbf{k}}^{\text{LDA}*}(\mathbf{r}_1) \\ & \times \{ \Delta [V_{xc}(\mathbf{r}_1)(1 - Z_{n\mathbf{k}})] \delta(\mathbf{r}_1 - \mathbf{r}_2) \\ & + \Delta [Z_{n\mathbf{k}} \Sigma(\mathbf{r}_1, \mathbf{r}_2, E_{n\mathbf{k}}^{\text{LDA}})] \} \phi_{n\mathbf{k}}^{\text{LDA}}(\mathbf{r}_2) d\mathbf{r}_1 d\mathbf{r}_2 \end{aligned} \quad (12)$$

the $\phi_{n\mathbf{k}}^{\text{LDA}}$ is the LDA wave function calculated for the initial cluster, $n\mathbf{k}$ is the LC or HV state, the changes V_H , V_{xc} , $Z_{n\mathbf{k}}$, and Σ arise from modification of the occupation factors $f_{n\mathbf{k}}$ in charged clusters. The calculation of electronic structure by the supercell method requires a special attention to charge neutrality. Charging each cell in the periodic structure provides diverging contribution to V_H . To remove this unphysical contribution in charged clusters, we placed a neutralizing charge at a spherical surface around the cluster. This construction cancels the diverging terms of V_H and changes potential inside the cluster by a constant. The constant does not affect the physical characteristics of the cluster and can be omitted for simplicity. To obtain charge neutrality in charged bulk silicon, we added a uniform positive background, as it was made in early studies.^{7,8} The Coulomb potential of this background perfectly compensates the average Hartree po-

tential of additional electrons so in this case the term V_H in Eq. (12) gives practically zero contribution and can be neglected. Therefore the shift of the lowest conduction ΔE_{LC} and highest valence ΔE_{HV} states in bulk silicon, induced by additional electrons in the conduction band is given by

$$\begin{aligned} \Delta E_{n\mathbf{k}}^{\text{QP}} = & \int \phi_{n\mathbf{k}}^{\text{LDA}*}(\mathbf{r}_1) \{ \Delta [V_{xc}(\mathbf{r}_1)(1 - Z_{n\mathbf{k}})] \delta(\mathbf{r}_1 - \mathbf{r}_2) \\ & + \Delta [Z_{n\mathbf{k}} \Sigma(\mathbf{r}_1, \mathbf{r}_2, E_{n\mathbf{k}}^{\text{LDA}})] \} \phi_{n\mathbf{k}}^{\text{LDA}}(\mathbf{r}_2) d\mathbf{r}_1 d\mathbf{r}_2. \end{aligned} \quad (13)$$

Here the $\phi_{n\mathbf{k}}^{\text{LDA}}$ is the LDA wave function obtained for intrinsic bulk silicon, $n\mathbf{k}$ is the LC or HV state.

III. BULK SILICON

The carrier induced band-gap narrowing in bulk silicon was studied both experimentally^{3,4} and theoretically.⁵⁻⁸ In experiment additional electrons may be introduced into bulk silicon by injection with an applied voltage or by impurity doping. In bulk silicon charged by electron injection additional electrons change the electron-electron interaction that results in gap narrowing.⁸ In doped bulk silicon besides this mechanism the gap decreases also because of the electron-donor scattering. In this section we consider the effect of electron charging on the gap of bulk silicon and particular mechanisms of the gap narrowing. There are two basic reasons for change in the electron-electron interaction under charging.⁵⁻⁸ The first reason is the screened exchange interaction between additional electrons, which decreases the energy of the conduction band minimum. The effect of this interaction on the valence-band maximum is weaker because of orthogonality of the wave functions on either side of the gap. As a result, the gap decreases. The second reason is an extra screening of the electron-electron interaction by additional electrons. The screened exchange interaction between electrons in the valence band tends to increase the gap by lowering the energy of the valence-band maximum. The extra screening decreases the screened exchange interaction between electrons and results in the gap narrowing. We note that in bulk silicon additional electrons partially occupy the conducting band and their contribution to the screening is of a metallic type. Therefore this mechanism of gap narrowing is very efficient and was considered in Ref. 8 as the basic one.

In this section we calculate the band gap narrowing in bulk silicon in the first-order perturbation theory and including the renormalization factor $Z_{n\mathbf{k}}$. Charge-induced shifts of the conduction-band minimum and valence-band maximum are evaluated according to Eq. (12), where changes ΔV_H , ΔV_{xc} , $\Delta Z_{n\mathbf{k}}$, and $\Delta \Sigma$ are due to modification of the occupation factors $f_{n\mathbf{k}}$ after the charging. Our *ab initio* calculation performed on a regular $18 \times 18 \times 18$ mesh in the reciprocal space provides all necessary information about the electronic structure of bulk Si, therefore experimental data on the static dielectric constant and effective masses were not used. The valence-band maximum and conduction-band minimum were taken at $(0, 0, 0)2\pi/a$ and $(0, 0, 0.889)2\pi/a$ \mathbf{k} points correspondingly, where $a=5.431$ Å is the experimental value of the lattice parameter. The computed GW indirect

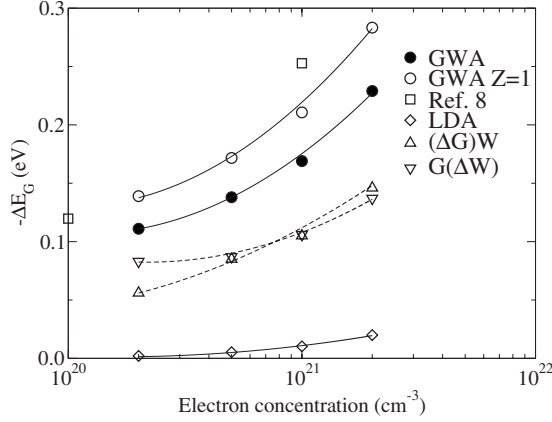


FIG. 1. Calculated gap narrowing in bulk silicon within the GWA including the renormalization factor Z (filled circles) and with $Z=1$ (open circles), and within the LDA (diamonds). The gap narrowing calculated within the GWA in Ref. 8 ($Z=1$) is shown by squares. Contributions to the change in the self-energy from $(\Delta G)W$ and $G(\Delta W)$ operators are shown by up and down triangles correspondingly. The lines are drawn as a guide for the eye.

gap in bulk silicon is 1.13 eV that is slightly smaller than the experimental value 1.17 eV. The calculated gap narrowing monotonically depends on concentration of additional electrons (Fig. 1), as it was observed in early calculations.⁸ Its absolute value is close to that from Ref. 8 (to be compared to our calculation with $Z=1$). The LDA calculation of the Kohn-Sham gap gives a much smaller gap narrowing (Fig. 1), so, as it was concluded in Ref. 8, the LDA is wholly inadequate to such an effect description.

It is interesting to compare the two mechanisms contributing to the total gap narrowing, which, arises essentially from a change in the self-energy operator upon electron charging. This change can be symbolically represented as a sum of two operators⁸

$$\Delta(GW) = (\Delta G)W^{int} + G^{ch}(\Delta W). \quad (14)$$

The first term in the right-hand side of Eq. (14) is the contribution of additional electrons to the screened exchange interaction between electrons. As has been discussed above, because of wave function orthogonality, this term stronger affects the LC than the HV state. The screened Coulomb interaction of the intrinsic bulk silicon W^{int} remains unchanged in this mechanism. The second term contains the Green's function of the charged silicon G^{ch} and a change in the screened interaction caused by additional electrons. This term mainly affects the HV state. Our calculation shows (Fig. 1) that relative values of gap narrowing arising from $(\Delta G)W^{int}$ and $G^{ch}(\Delta W)$ are, respectively, 52% and 48% at the concentration of additional electrons $2.0 \times 10^{21} \text{ cm}^{-3}$. This result shows that contributions of the both mechanisms to the narrowing effect are important and should be explicitly taken into account.

IV. SILICON CLUSTERS

A. Initial cluster

The charged and doped clusters studied in the next sections are based on an initial silicon cluster which contains 35

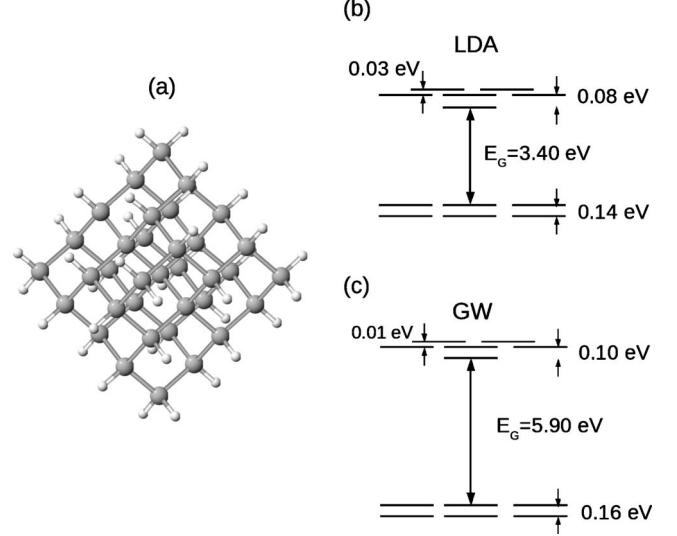


FIG. 2. (a) Initial $\text{Si}_{35}\text{H}_{36}$ cluster and its electronic structure calculated within the (b) LDA and (c) GWA at the Γ point (a few conduction and valence states are shown).

silicon atoms [Fig. 2(a)]. The initial cluster is centered on a Si atom and has the T_d symmetry. The effective diameter of the cluster is 1.1 nm, as calculated from the volume of one Si atom in bulk silicon, multiplied by the number of atoms in the cluster.

The surface dangling bonds were saturated by 36 hydrogen atoms to eliminate surface electronic states from the gap. This is important because the surface states could capture additional electrons introduced by impurity doping or injected by applied voltage and modify the intrinsic gap-narrowing effect. This $\text{Si}_{35}\text{H}_{36}$ cluster was then placed inside the primitive cell of the cubic face-centered lattice. The lattice parameter of the cell was chosen sufficiently large to ensure a good vacuum separation between the periodical replicas in neighbor supercells. The minimum distance between atoms of clusters in neighbor supercells was kept to be 9 Å. The initial cluster was relaxed using the LDA electronic-structure calculation and the Broyden-Fletcher-Goldfarb-Shanno scheme.²⁶ The reciprocal space was sampled at the Γ point. A calculation performed on a finer $2 \times 2 \times 2$ \mathbf{k} mesh provides negligible changes to the atomic structure of the initial cluster relaxed using the sampling at the Γ point. The relaxation does not change T_d symmetry of the initial cluster,^{27,28} however obtained interatomic Si-Si distances are larger in the center (2.33 Å) and smaller on the surface (2.32 Å) of the cluster. This tendency of bond length shortening from the center to surface was clearly observed in Si clusters of different sizes.²⁹

The electronic structure of the cluster was calculated within the GWA, on a regular mesh $2 \times 2 \times 2$ in the reciprocal space. The LDA and GW eigenvalues of the cluster calculated at the Γ point are schematically shown in Figs. 2(b) and 2(c), respectively (only a few conduction and valence states near the gap are shown). The calculated Kohn-Sham LDA gap is 3.40 eV, in agreement with previous calculations reporting 3.50 and 3.40 eV.^{30,31} The lowest conduction state is a singlet and within the GWA it is separated from a higher

threefold-degenerate conduction state by the energy interval 0.10 eV. The highest valence state is threefold degenerate. It is separated from a lower lying threefold-degenerate valence state by the interval 0.16 eV [Fig. 2(c)]. The GW gap is determined as an energy difference between the single LC and threefold-degenerate HV states, is 5.90 eV in the initial cluster, a value 5.4 eV for the quasiparticle gap was obtained in an *ab initio* real-space calculation.³² Developing the LDA wave functions over spherical harmonics around the cluster center, we found that the LC state contains 34% harmonics of the *s* symmetry and 0% of the *p* symmetry. In contrast, the threefold-degenerate HV state has no contribution of the *s* symmetry and contains 19% harmonics of the *p* symmetry. This agrees well with previous experimental¹⁰ and theoretical³³ investigations, pointing out to the *s* symmetry of the LC state in clusters. The energy bands of the cluster calculated with the supercell method are not absolutely flat, as energy levels of an isolated cluster should be. This artificial band width arises from the overlapping of wave functions from neighbor supercells. In the case of partial level occupation the band curvature may provide an intraband contribution to the dielectric matrix. This intraband contribution is absent in real isolated clusters, therefore it was suppressed in our calculation of the dielectric matrix in doped and charged clusters.

B. Charged clusters

Additional electrons in charged clusters are injected by an external voltage. In our calculation we suppose that there is a positive and homogeneously charged spherical surface around the cluster which neutralizes the supercell. In absolute values the charge of the sphere exactly equals to charge of the additional electrons. We assume also that the electron injection does not change the crystal structure of the cluster, since in this case there are no impurity atoms of different size, which shift neighboring cluster atoms from their positions.

The gap narrowing in charged clusters for different electron concentrations was calculated according to Eq. (11). In the first-order perturbation theory the shifts of the LC and HV states under charging can be evaluated from Eq. (12). The changes of the Hartree ΔV_H potential and of the exchange-correlation term $Z\Sigma + V_{xc}(1-Z)$ in Eq. (12) were computed by modifying the electron occupation factors of the initial cluster. Four different charges of the cluster were considered: $-2e$, $-1e$, $-0.5e$, and $-0.2e$. These charges correspond to electron concentrations $2.9 \times 10^{21} \text{ cm}^{-3}$, $1.4 \times 10^{21} \text{ cm}^{-3}$, $7.1 \times 10^{20} \text{ cm}^{-3}$, and $2.9 \times 10^{20} \text{ cm}^{-3}$, respectively. Results obtained for two last concentrations have no direct physical application since a cluster cannot be charged by a rational number of electrons. In this paper they are used to trace the gap-narrowing behavior in a wider concentration interval.

First we evaluate the charge-induced gap narrowing of the cluster within the LDA. The shifts of the LC and HV states can be calculated using Eq. (12), where modification of the exchange-correlation term $\Delta[Z\Sigma + V_{xc}(1-Z)]$ is replaced by a modification of the exchange-correlation potential

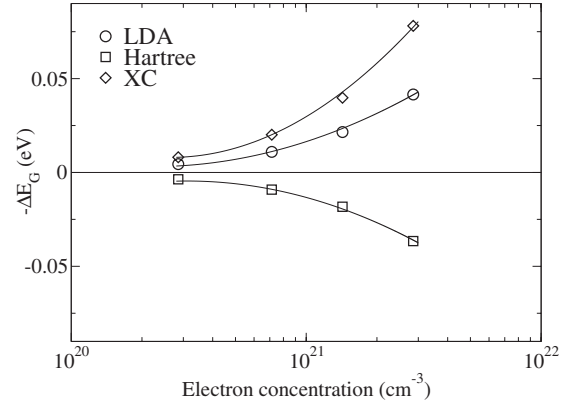


FIG. 3. The gap narrowing in charged $\text{Si}_{35}\text{H}_{36}$ cluster as a function of electron concentration. The LDA gap narrowing (circles) is calculated as a sum of contributions from the Hartree potential (squares) and the exchange-correlation potential (diamonds). The solid lines are drawn as a guide for the eye.

$\Delta V_{xc}(\mathbf{r}_1)\delta(\mathbf{r}_1-\mathbf{r}_2)$. Calculated contributions to the gap narrowing from the Hartree and exchange-correlation potentials are shown in Fig. 3. The Hartree contribution increases the gap, as it was observed in bulk silicon: additional electrons in the LC state increase the electrostatic energy of this state, while their effect on the HV state is weaker because of smaller overlap between the additional and HV-electron densities. The exchange-correlation contribution decreases the gap since the potential ΔV_{xc} acts in the opposite direction: the negative exchange-correlation potential of additional electrons decreases the energy of the LC and HV states, and this effect is smaller for the HV state. The exchange-correlation contribution to gap narrowing exceeds the Hartree one and within the LDA the gap slightly decreases upon electron charging (Fig. 3). The same trend was observed in bulk silicon.⁸

In order to evaluate the gap narrowing in charged clusters within the GWA, the shifts of the LC and HV states were computed according to Eq. (12). The calculated contribution due to the change in the self-energy $\Delta\Sigma$ clearly decreases the gap (Fig. 4) and the gap narrowing in clusters arises essentially from the self-energy modification. The mechanisms which lead to a negative contribution of the self-energy to the gap are the same as in the bulk silicon. The first mechanism is the screened exchange interaction between the additional electrons in the LC state. An additional charge increases the Hartree energy of both LC and HV states, they almost rigidly shift upward in energy. The screened exchange interaction between additional electrons lowers the LC and HV states downward in energy but the energy shift of the HV state is smaller because of orthogonality of the LC and HV states. The second mechanism relates to screening increase induced by the additional electrons. Interaction between valence electrons tends to increase the gap. This interaction is more efficiently screened in the presence of additional electrons that leads to the gap narrowing. Quantitatively, contribution of the mechanisms can be evaluated from Eq. (14). We have found that relative contributions of $(\Delta G)W^{int}$ and $G^{ch}(\Delta W)$ to the gap narrowing were, respectively, 83% and 17% at the electron concentration $2.9 \times 10^{21} \text{ cm}^{-3}$, against

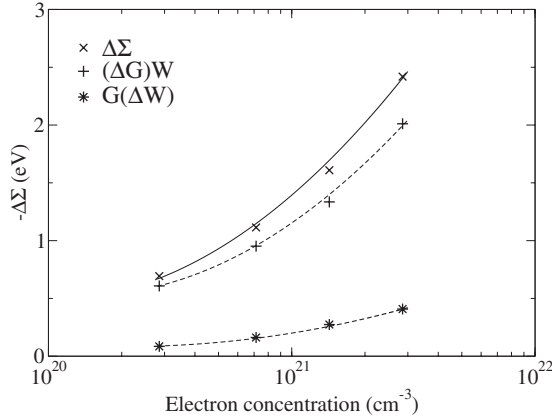


FIG. 4. The change in self-energy as a function of electron concentration in charged clusters (crosses). Contributions to the change in the self-energy from $(\Delta G)W$ and $G(\Delta W)$ operators are shown by pluses and stars, respectively. The solid lines are drawn as a guide for the eye.

52% and 48% in bulk silicon at the concentration $2.0 \times 10^{21} \text{ cm}^{-3}$. This difference between bulk Si and the Si cluster is explained by two factors. First, a lower dielectric function leads to stronger screened exchange interaction in the Si cluster than in bulk Si that provides larger $(\Delta G)W^{int}$ contribution. Second, the conduction states of the cluster has a discrete energy structure, therefore extra screening caused by additional electrons is of a dielectric type. In bulk Si additional electrons provide metallic type screening, which stronger reduces the Coulomb interaction of electrons comparing to the cluster. By this reason in the cluster the contribution $G^{ch}(\Delta W)$ is smaller.

A comparison of the total gap narrowing in the $\text{Si}_{35}\text{H}_{36}$ cluster calculated within the GWA (Fig. 5) and LDA (Fig. 6) shows that the LDA gives a highly underestimated result for the charge induced gap narrowing. The LDA therefore is inadequate to describe such effects in silicon clusters. The same conclusion was earlier made for bulk silicon.⁸

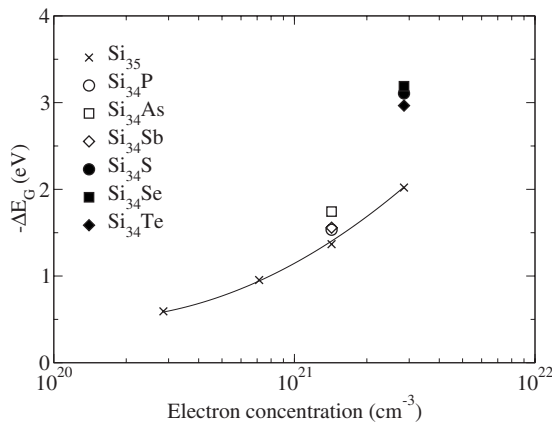


FIG. 5. The total GW gap narrowing in charged (crosses) and doped (symbols) clusters. Open and filled symbols correspond to a single- and double-donor doping, respectively. The solid lines are drawn as a guide for the eye.

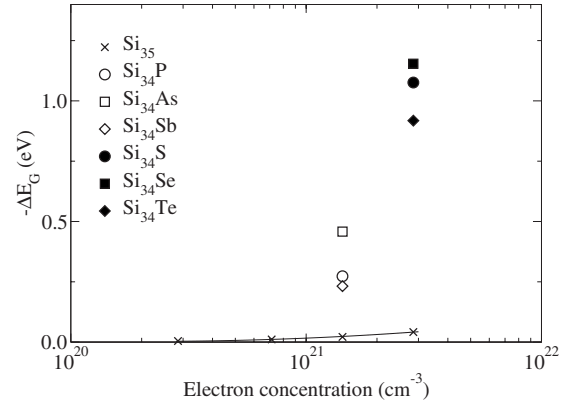


FIG. 6. The total LDA gap narrowing in charged (crosses) and doped (symbols) clusters. Open and filled symbols correspond to a single- and double-donor doping, respectively. The solid lines are drawn as a guide for the eye.

C. Doped clusters

Doped silicon clusters were constructed from the initial cluster, replacing the central Si atom by an impurity atom. Then the structural relaxation of atomic positions in the clusters was performed using a nonspin-polarized LDA calculation. In general, this relaxation may change the cluster symmetry. For example, the lower C_{3v} symmetry was found in small Si clusters doped with B and N.^{33,34} The doping leads to the different distances between the impurity atom and its four nearest-neighbor (nn) Si atoms that lowers the symmetry. Previous LDA calculations^{33,34} show that the T_d symmetry remains unchanged in P-, As-, and Sb-doped Si nanoclusters. In our calculation we impose the T_d symmetry to the doped clusters and relax the atomic positions for the fixed symmetry. The same T_d symmetry of the initial, charged, and doped clusters reduces computing time and allows discussing electronic structure of all clusters in common terms. The calculated displacements are small only for P doping while for As, Sb, S, Se, and Te they are between 0.1 and 0.4 Å, as one can see from Table I.

Doping of the cluster introduces additional electrons in the LC state and changes the crystal potential near the cluster center. The mechanisms of the gap narrowing induced by the additional electrons are essentially the same as in charged silicon clusters. The new factor is a different crystal potential of the central atom. It causes atomic relaxation discussed above and strongly localizes additional electrons near the cluster center. For example, the probability that an additional electron is inside a sphere of the radius 2.35 Å located at the cluster center is only 7.8% for the uniform electron distribution but it exceeds 30% for the S- and Se-doped clusters (Table I). This factor significantly affects the LDA results and increases contribution of the self-energy operator. In doped Si clusters the LDA gap narrowing is significantly larger than in the charged clusters (Fig. 6). For example, the LDA gap of $\text{Si}_{34}\text{PH}_{36}$ is 3.13 eV, a similar value was obtained in Ref. 34. The resulting LDA gap narrowing is 0.27 eV, that is significantly larger than 0.02 eV in the single-electron charged cluster. According to our calculation the most important contribution to the narrowing in the doped

TABLE I. List of parameters for doped and charged clusters: distance between the central atoms and its nearest neighbor atom; contribution to the gap narrowing arising from modification of all operators in Eq. (2) excepting the self-energy; exchange-correlation contribution to the gap narrowing from the $V_{xc}(1-Z)+Z\Sigma$ operator in Eq. (12); localization of the LC electron near an impurity atom (probability to find an electron inside a sphere around the central atom, the sphere radius is 2.35 Å).

Impurity or charge	Central atom-nn distance (Å)	Contribution $-\frac{1}{2}\nabla^2+V_{ext}+V_H$ (eV)	Exch.-corr. contribution (eV)	Localization near impurity
Charge= $-1e$	2.33	0.018	-1.386	0.096
P	2.31	0.055	-1.589	0.203
As	2.41	-0.023	-1.721	0.241
Sb	2.54	-0.068	-1.490	0.153
Charge= $-2e$	2.33	0.037	-2.057	0.096
S	2.44	-0.148	-2.958	0.333
Se	2.56	-0.333	-2.856	0.316
Te	2.71	-0.257	-2.708	0.262

clusters is due to a large modification of the exchange-correlation potential while the common contribution of other operators in Eq. (1) is smaller. This is the effect of localization of additional electrons near the positive charged impurity ion, which increases the exchange energy between the additional electrons and move the LC state downward in energy. This explains the significant difference between the LDA results obtained in doped and charged clusters. The LDA gap narrowing calculated in $Si_{34}DH_{36}$ clusters for single ($D=P, As, Sb$) and double ($D=S, Se, Te$) donors (Fig. 6) is much smaller than the GWA result (Fig. 5) so an inadequacy of LDA computation is evident. One can see that the GWA gap narrowing calculated for different single-donor impurities is nearly equal, though a small dispersion of results exists. A small dispersion of the narrowing results is also observed in double-donor doped clusters. The origin of this dispersion is again the localization of additional electrons, which depends not only on the charge of impurity ion, but also on its chemical nature. A more detailed consideration of mechanisms which are responsible for the gap narrowing in the charged and doped Si clusters is given in the next section.

V. DISCUSSION

Mechanisms of the gap narrowing in charged nanoclusters. Our *ab initio* computation performed for neutral and n -type charged bulk Si, for the neutral, $-1e$, and $-2e$ -charged $Si_{35}H_{36}$ clusters, as well as for the doped $Si_{34}DH_{36}$ ($D=P, As, Sb, S, Se, Te$) clusters, provides us with a rich information for the analysis of carrier-induced gap narrowing in semiconducting nanoclusters. As the LDA calculation does not reproduce correctly this effect, the main contributions to $\Delta\Sigma$ should be considered. As compared to bulk Si, the $Si_{35}H_{36}$ cluster has three important features, which affect its gap narrowing caused by charging or doping. First, the $Si_{35}H_{36}$ cluster has a much larger gap ($E_G=5.90$ eV vs. 1.17 eV in bulk Si). This hampers electronic excitations across the gap (from occupied valence to empty conduction states) and therefore the electronic response in the cluster is significantly weaker. Second, because of finite

size, conduction states in clusters consist of discrete electron levels, while the conduction band of bulk Si has a continuous spectrum. By this reason, the extra screening by additional electrons is of the dielectric type in $Si_{35}H_{36}$ and of the metallic type in bulk Si that reduces its value and relative importance in clusters. Third, a finite size of the cluster strongly affects its screening properties. This problem has been discussed in several publications.³⁵⁻³⁹ If external electric field is created by a positive point charge Q placed in the center of the cluster, electrons in the cluster move to the charge and screen the external field by this way. Because of the total charge conservation, the increase of the electron density near the cluster center must be compensated by electron deficit near the cluster surface. For this reason electron response near the cluster surface is of the antiscreening type. Beyond the spherical cluster the screened field of Q coincides with the unscreened one since the both fields are produced just by the external charge Q . This means that the effective dielectric function is unit at the cluster surface and remains close to unit near the surface inside the cluster. This effect greatly decreases the effective dielectric function related to the Coulomb interaction of charges in the cluster. For example, the exciton Coulomb energy in the $Si_{35}H_{36}$ cluster is characterized by the average dielectric constant $\epsilon_{ave}=1.33$, which describes the screened interaction between conduction electrons with $\rho(\mathbf{r})=|\psi_{LC}(\mathbf{r})|^2$ and valence holes with $\rho(\mathbf{r})=|\psi_{HV}(\mathbf{r})|^2$.³⁷ The situation is essentially different in the case of the homogeneous external field $\mathbf{E}_{ext}(\mathbf{r})=const$. The total charge conservation does not impose limitation to the value of induced dipole moment in the cluster, therefore the external field $\mathbf{E}_{ext}(\mathbf{r})$ is screened more efficiently than the point charge field. For example, the static dielectric constant of the $Si_{35}H_{36}$ cluster is $\epsilon_0=4.4$.^{32,40} The present calculation correctly reproduces these finite-size effects of screening in clusters. For screened Coulomb interaction of additional electrons with $\rho(\mathbf{r})=|\psi_{LC}(\mathbf{r})|^2$ related to $\Delta\Sigma$ our average dielectric constant is $\epsilon_{ave}(\Delta\Sigma)=1.38$ while our static dielectric constant estimated from the diagonal Fourier element $\epsilon_{00}^{-1}(\mathbf{q}=0, E=0)$ is $\epsilon_0=4.1$. These facts show that screening in the cluster is much weaker than in bulk Si ($\epsilon_0=11.4$).

All the three features considered above indicate that in clusters the role of extra screening by additional electrons is

significantly lowered while the role of the screened exchange is much increased. These trends are seen from Figs. 1 and 4, where the contributions to $\Delta\Sigma$ from the screened exchange between additional electrons and the extra screening of Coulomb interaction are presented for n -type charged bulk Si and $\text{Si}_{35}\text{H}_{36}$. They show that the screened exchange between additional electrons is the dominant mechanism of gap narrowing in the charged $\text{Si}_{35}\text{H}_{36}$ nanoclusters.

Charge localization near impurity ion. If one compares the calculated GWA gap narrowing for doped and charged clusters, one can see that the narrowing effect is more pronounced in doped than in charged clusters (Fig. 5). The difference is smaller for clusters doped with single donors and charged by a single electron but it becomes considerable in the case of double donor doping and charging by a pair of electrons. Doping creates a positive charged impurity ion inside the cluster, together with a distortion of crystal structure around the ion, and hence alters the external V_{nk}^{ext} potential, LDA wave functions ϕ_{nk}^{LDA} and eigenvalues E_{nk}^{LDA} in Eq. (1). In particular, the electron charge is localized around the positive charged impurity ions. The altered wave functions and eigenvalues are further used to construct the Hartree potential and self-energy in Eq. (2). In doped clusters the total effect of gap narrowing arises from the change in the Hartree and external potentials, self-energy and also from modification of the LDA wave functions. In charged clusters the electron wave functions are taken to be unchanged. The positive charged sphere around the charged cluster creates a constant potential inside itself and it does not modify the gap. Therefore the total effect of gap narrowing in charged clusters arises from modification of the Hartree potential and self-energy only. In order to understand the nature of different gap narrowing in doped and charged clusters we separate contribution from the self-energy and other operators in Eq. (2). One can see from Table I that the difference in gap narrowing between doped and charged clusters is essentially due to the self-energy. If we evaluate the self-energy contribution to the gap narrowing within the Hartree-Fock approximation [in this case the screened potential W in Eq. (5) is replaced by the bare Coulomb potential] then we again obtain larger contributions to the gap narrowing in doped clusters. This suggests that the difference is not related to a change of screening and originates from localization of LC-wave function near the positive charged impurity ion in doped clusters. Such a localization increases the exchange interaction between electrons in the LC state and leads to a larger gap narrowing in doped cluster as compared to charged one. In order to evaluate the localization of the LC-wave function, the probability of LC electron to be inside a sphere around the impurity ion was calculated. The sphere radius was chosen to be equal to the interatomic distance in bulk silicon (2.35 Å). The probabilities for doped and charged clusters are listed in Table I. One can see that the self-energy contribution to the gap narrowing correlates directly to the calculated probabilities: the more the LC electron is localized near the impurity ion, the more the contribution of the self-energy to the gap narrowing. Thus the hypothesis of strong localization of the LC electron near impurity ion explains well the large difference in gap narrowing between doped and charged clusters.

Large cluster limit. It is important to generalize these results to larger nanoclusters, which are usually fabricated for experimental research. Large clusters require enormous computer resources, which presently hinders direct GWA calculations. The fact that the screened exchange between additional electrons is the main mechanism of gap narrowing in the Si:H clusters of 1.1 nm diameter greatly simplifies effect consideration. As cluster size d grows, the carrier concentration introduced by one additional electron decreases and the exchange contribution to the self-energy operator decreases approximately as $1/d$. A smaller concentration of additional electrons also reduces the extra screening of Coulomb interaction relating to the second mechanism of gap narrowing. Both these changes were taken into account in our GWA calculation performed for the $\text{Si}_{35}\text{H}_{36}$ cluster charged by a fractional electron number $0.2e$ and $0.5e$, which may be related conditionally to the Si:H clusters with the diameter 1.4 nm and 1.9 nm, respectively (Figs. 4 and 5). But larger clusters have as well a smaller gap and a stronger screening of the exchange interaction between additional electrons. Moreover, the conduction band of large clusters has a denser discrete spectrum that increases the efficiency of extra screening by additional electrons. These factors are beyond our GWA calculation with fractional occupation numbers, therefore concentration dependence presented in Fig. 4 can be considered only as an upper estimate of gap narrowing. This estimate may be improved further, if the factor $\epsilon(\text{Si}_{35}\text{H}_{36})/\epsilon(\text{Si:H})$, which corrects the screening of exchange between additional electrons in a Si:H cluster, is taken into account. From this point of view a larger gap narrowing calculated for doped $\text{Si}_{34}\text{DH}_{36}$ clusters, as compared to charged ones relating to formally equal electron concentrations, can be treated as the result of a higher effective concentration of additional electrons caused by their localization near the impurity atom.

Gap narrowing and spin splitting. All calculations presented above ignored electron spins. Since the clusters $\text{Si}_{35}\text{H}_{36}$ with the charge $-1e$ and $\text{Si}_{34}\text{DH}_{36}$ ($D=\text{P, As, Sb}$) have an odd number of electrons, the spin moment of these clusters is not zero. As a result, the LC states related to different spin projections should be split in energy. Below we discuss this effect by taking as an example the single electron charged cluster. In general charging may reduce the symmetry of cluster due to for example the Jahn-Teller distortion. In this estimate we assume, as before, that the charging does not alter the atomic positions, which are those of the initial $\text{Si}_{35}\text{H}_{36}$ cluster. Our spin-polarized calculation performed within the local spin-density approximation gives the LC energy splitting $E^{\text{LSDA}}(\text{LC})=E_{\downarrow}-E_{\uparrow}$ only 0.08 eV (here and below electron states with spin up relate to the majority spin projection). The spin splitting of this order (between 0.1 and 0.3 eV) has been calculated earlier within the generalized-gradient approximation to the density functional theory in the Si nanoclusters of 1 nm in diameter doped by B, N, Al, and P atoms.³⁴ As it was shown above, the screened exchange interaction between additional electrons gives the main contribution to the gap narrowing. For this reason we restrict our further consideration of spin effects to the HF and screened Hartree-Fock (SHF) approximations. Within the HF method, occupation of the spin-up LC state by one electron

changes only the self-energy operator Σ_{\uparrow} while $\Delta\Sigma_{\downarrow}$ is zero. For this reason the energy $E_{\uparrow}^{\text{HF}}(\text{LC})$ is greatly lowered by $\Delta\Sigma_{\uparrow}$ while $E_{\downarrow}^{\text{HF}}(\text{LC})$ remains unchanged by $\Delta\Sigma_{\downarrow}$ that provides a significant spin splitting of the LC states. At the same time, the spin splitting of the HV states caused by a spin moment of LC electrons should be rather weak because of the orthogonality between conducting and valence states. Our spin-polarized HF calculation shows that the splitting of the LC states is as large as $E_{\downarrow}^{\text{HF}}(\text{LC}) - E_{\uparrow}^{\text{HF}}(\text{LC}) = 3.04$ eV, while the splitting of the HV states is only $E_{\downarrow}^{\text{HF}}(\text{HV}) - E_{\uparrow}^{\text{HF}}(\text{HV}) = 0.09$ eV. By this means, in the HF approximation the gap narrowing caused by $-1e$ charging is 2.95 eV for spin-up electron transitions and 3.04 eV for spin-flip electron transitions. For comparison, the HF gap narrowing calculated without spin polarization is 1.95 eV so the inclusion of electron spins increases the spin-up gap narrowing by 1.00 eV. A more precise estimate of spin splitting and gap narrowing can be obtained within the SHF approximation. As electron screening weakly depends on spin polarization, required dielectric constants can be taken from our nonmagnetic GWA calculation. This gives $E_{\downarrow}^{\text{SHF}}(\text{LC}) - E_{\uparrow}^{\text{SHF}}(\text{LC}) = [E_{\downarrow}^{\text{HF}}(\text{LC}) - E_{\uparrow}^{\text{HF}}(\text{LC})] / \epsilon_{\text{ave}} = 2.20$ eV, where the average effective dielectric constant $\epsilon_{\text{ave}} = 1.38$ relates to the Coulomb interaction between additional electrons with $\rho(\mathbf{r}) = |\psi_{\text{LC}}(\mathbf{r})|^2$. The spin splitting of the HV states is estimated as: $E_{\downarrow}^{\text{SHF}}(\text{HV}) - E_{\uparrow}^{\text{SHF}}(\text{HV}) = [E_{\downarrow}^{\text{HF}}(\text{HV}) - E_{\uparrow}^{\text{HF}}(\text{HV})] / \epsilon_0 = 0.02$ eV. Here the effect of screening is described with the static dielectric constant $\epsilon_0 = 4.1$, which is more suitable for screened Coulomb interaction of the dipoles $\psi_{\text{LC}}(\mathbf{r})\psi_{\text{HV}}(\mathbf{r})$ in the cluster [because of the orthogonality between valence and conducting states the integral of $\psi_{\text{LC}}(\mathbf{r})\psi_{\text{HV}}(\mathbf{r})$ taken over the cluster is zero, therefore the product $\psi_{\text{LC}}(\mathbf{r})\psi_{\text{HV}}(\mathbf{r})$ is treated just as a dipole, but not as a charge]. As a result, the gap narrowing in the single electron charged $\text{Si}_{35}\text{H}_{36}$ cluster caused by ΔG is about 2.18 eV for spin-up electron transitions and 2.20 eV for spin-flip transitions while without spin-polarization it is only 1.34 eV (Fig. 4). The presented estimates show that in small semiconducting clusters with an odd number of electrons the effects of spin polarization are very important. They cause a large spin splitting of the LC states, which is of the same order as the total gap narrowing, and a significant extra narrowing of the gap. The density-functional theory does not describe adequately these effects. An accurate estimate of the effects of spin polarization is difficult in large clusters since such a computation is too time consuming. However a general decrease of the spin effects with growing cluster size is evident. In our opinion, these effects remain observable in clusters of 3–5 nm in size. Apropos of this, a doublet split-

ting of 0.25 eV measured by scanning tunneling microscopy was reported in the InAs quantum dots of $d = 2.8$ nm.¹⁰ The existence of so significant spin splitting in nanoclusters with an odd number of electrons makes possible optical orientation of spins and may be of interest for spintronics.

VI. CONCLUSION

The gap narrowing in charged and n -type doped silicon nanoclusters was calculated within the GW approximation. We show that this effect cannot be properly evaluated from a calculation of the Kohn-Sham LDA gap in nanoclusters, since such a calculation greatly underestimates the gap narrowing. Although the basic mechanisms of gap narrowing in charged and doped clusters are the same, as in bulk silicon, their relative contributions are very different. We found the equal importance of two mechanisms in bulk Si, namely, of (i) the screened exchange interaction between additional electrons and (ii) the extra screening of Coulomb interaction caused by additional electrons. In nanoclusters the first mechanism is dominant. Its contribution increases further in doped clusters because of the localization of conducting electrons near the impurity atom. In the clusters with an odd number of electrons the electron spectrum is spin split. A calculation performed with the screened Hartree-Fock method shows that the LC spin splitting is large and even exceeds the nonmagnetic gap narrowing arising from the screened exchange interaction. This effect is strongly underestimated in the LDA and also requires a quasiparticle description. The spin splitting leads to an additional narrowing of the gap and introduces spin effects into electronic properties of nanoclusters.

ACKNOWLEDGMENTS

We are grateful to V. Olevano and H. Mera for numerous discussions, and to M. Giantomassi for his replies at the ABINIT forum. Calculations were performed at the cluster MERLIN of the IM2NP-France and at supercomputer centers of the RSC “Kurchatov Institute” and of the Russian Academy of Sciences in Moscow. Authors acknowledge the financial support of the French Research Agency (Project No. MEMOIRE 05-NANO-043), Russian Foundation for Basic Research (Programs No. 09-02-91078-CNRS-a; No. 10-02-00118-a; and No. 10-02-00698-a) and of the Russian Academy of Sciences (programs “Strongly correlated electrons in solids and structures,” “Basic investigations of nanotechnologies and nanomaterials”).

*titov@nsc.gpi.ru

†fabienne.michelini@univ-provence.fr

‡uspenski@td.lpi.ru

¹H. Sliva, M. K. Kim, U. Avci, A. Kumar, and S. Tiwari, *MRS Bull.* **29**, 845 (2004).

²D. D. Tang, *IEEE Trans. Electron Devices* **27**, 563 (1980).

³P. E. Schmid, *Phys. Rev. B* **23**, 5531 (1981).

⁴J. Wagner, *Phys. Rev. B* **32**, 1323 (1985).

⁵J. C. Inkson, *J. Phys. C* **9**, 1177 (1976).

⁶K.-F. Berggren and B. E. Sernelius, *Phys. Rev. B* **24**, 1971 (1981).

⁷R. Abram, G. N. Childs, and P. A. Saunderson, *J. Phys. C* **17**,

- 6105 (1984).
- ⁸A. Oschlies, R. W. Godby, and R. J. Needs, *Phys. Rev. B* **51**, 1527 (1995).
- ⁹H. Drexler, D. Leonard, W. Hansen, J. P. Kotthaus, and P. M. Petroff, *Phys. Rev. Lett.* **73**, 2252 (1994).
- ¹⁰U. Banin, Y. W. Cao, D. Katz, and O. Millo, *Nature (London)* **400**, 542 (1999).
- ¹¹K. H. Schmidt, G. Medeiros-Ribeiro, and P. M. Petroff, *Phys. Rev. B* **58**, 3597 (1998).
- ¹²R. J. Warburton, C. S. Durr, K. Karrai, J. P. Kotthaus, G. Medeiros-Ribeiro, and P. M. Petroff, *Phys. Rev. Lett.* **79**, 5282 (1997).
- ¹³A. Wojs and P. Hawrylak, *Phys. Rev. B* **55**, 13066 (1997).
- ¹⁴A. Franceschetti and A. Zunger, *Phys. Rev. B* **62**, R16287 (2000).
- ¹⁵L. Hedin, *Phys. Rev.* **139**, A796 (1965).
- ¹⁶The ABINIT code is a common project of the Université Catholique de Louvain, Corning Incorporated, and other contributors (URL <http://www.abinit.org>); M. C. Payne, M. P. Teter, D. C. Allan, T. A. Arias, and J. D. Joannopoulos, *Rev. Mod. Phys.* **64**, 1045 (1992); X. Gonze *et al.*, *Z. Kristallogr.* **220**, 558 (2005); *Comput. Phys. Commun.* **180**, 2582 (2009).
- ¹⁷N. Troullier and J. L. Martin, *Solid State Commun.* **74**, 613 (1990).
- ¹⁸A. Khein, *Phys. Rev. B* **51**, 16608 (1995).
- ¹⁹D. C. Allan and M. P. Teter, *Phys. Rev. Lett.* **59**, 1136 (1987).
- ²⁰S. de Gironcoli, *Phys. Rev. B* **51**, 6773 (1995).
- ²¹M. S. Hybertsen and S. G. Louie, *Phys. Rev. B* **34**, 5390 (1986).
- ²²R. W. Godby, M. Schlüter, and L. J. Sham, *Phys. Rev. B* **37**, 10159 (1988).
- ²³W. G. Aulbur, L. Jönsson, and J. W. Wilkins, *Solid State Phys.* **54**, 1 (1999).
- ²⁴S. L. Adler, *Phys. Rev.* **126**, 413 (1962).
- ²⁵N. Wiser, *Phys. Rev.* **129**, 62 (1963).
- ²⁶H. B. Schlegel, *J. Comput. Chem.* **3**, 214 (1982).
- ²⁷F. Iori, E. Degoli, R. Magri, I. Marri, G. Cantele, D. Ninno, F. Trani, O. Pulci, and S. Ossicini, *Phys. Rev. B* **76**, 085302 (2007).
- ²⁸Z. Zhou, R. A. Friesner, and L. Brus, *J. Am. Chem. Soc.* **125**, 15599 (2003).
- ²⁹H. Ch. Weissker, J. Furthmüller, and F. Bechstedt, *Phys. Rev. B* **67**, 245304 (2003).
- ³⁰E. Degoli, G. Cantele, E. Luppi, R. Magri, D. Ninno, O. Bisi, and S. Ossicini, *Phys. Rev. B* **69**, 155411 (2004).
- ³¹M. Luppi and S. Ossicini, *Phys. Rev. B* **71**, 035340 (2005).
- ³²S. Ögüt, J. R. Chelikowsky, and S. G. Louie, *Phys. Rev. Lett.* **79**, 1770 (1997).
- ³³Z. Zhou, M. L. Steigerwald, R. A. Friesner, L. Brus, and M. S. Hybertsen, *Phys. Rev. B* **71**, 245308 (2005).
- ³⁴L. E. Ramos, E. Degoli, G. Cantele, S. Ossicini, D. Nino, J. Furthmüller, and F. Bechstedt, *J. Phys.: Condens. Matter* **19**, 466211 (2007).
- ³⁵C. Delerue, M. Lannoo, and G. Allan, *Phys. Rev. B* **68**, 115411 (2003).
- ³⁶A. Franceschetti and M. C. Tropicovsky, *Phys. Rev. B* **72**, 165311 (2005).
- ³⁷S. Ögüt, R. Burdick, Y. Saad, and J. R. Chelikowsky, *Phys. Rev. Lett.* **90**, 127401 (2003).
- ³⁸D. Ninno, F. Trani, G. Cantele, K. J. Hameeuw, G. Iadonisi, E. Degoli, and S. Ossicini, *Europhys. Lett.* **74**, 519 (2006).
- ³⁹X. Cartoixa and L. W. Wang, *Phys. Rev. Lett.* **94**, 236804 (2005).
- ⁴⁰I. Vasiliev, S. Ögüt, and J. R. Chelikowsky, *Phys. Rev. Lett.* **78**, 4805 (1997).